HVAC&R Research

ISSN: 1078-9669 (Print) 1938-5587 (Online) Journal homepage: https://www.tandfonline.com/loi/uhvc20

Development, Evaluation, and Demonstration of a Virtual Refrigerant Charge Sensor

Haorong Li & James E. Braun

To cite this article: Haorong Li & James E. Braun (2009) Development, Evaluation, and Demonstration of a Virtual Refrigerant Charge Sensor, HVAC&R Research, 15:1, 117-136, DOI: 10.1080/10789669.2009.10390828

To link to this article: https://doi.org/10.1080/10789669.2009.10390828

Published online: 22 Feb 2011.

Development, Evaluation, and Demonstration of a Virtual Refrigerant Charge Sensor

Haorong Li, PhD
Member ASHRAE

James E. Braun, PhD
Fellow ASHRAE

Received July 29, 2008; accepted October 27, 2008

Proper refrigerant charge level is critical for vapor-compression cycle refrigeration systems to operate efficiently and safely. The current practice of accurately determining charge levels is very time consuming and costly. Technicians must stop and evacuate the system, weigh the removed charge, and add the correct amount of charge to the system using a scale. This paper presents a method for obtaining accurate estimates of refrigerant charge level using noninvasive temperature measurements obtained while the system is operating. The method could be used as part of a permanently installed control or monitoring system to indicate charge level and/or to automatically detect and diagnose low or high levels of refrigerant charge. It could also be used as a stand-alone tool by technicians to determine existing charge and during the process of adjusting the refrigerant charge. The accuracy of the virtual refrigerant charge sensor is evaluated using laboratory data for seven different systems and over a wide range of operating conditions with and without the presence of other faults. The evaluation and demonstration verify that the virtual refrigerant charge level gauge has very good performance in terms of accuracy and robustness and can be easily implemented and installed in terms of both hardware and software.

INTRODUCTION

A number of studies conducted by various independent investigators (Proctor and Downey 1995; Cowan 2004) have concluded that more than 50% of the packaged air-conditioning systems in the field were improperly charged due to improper commissioning, service, or leakage. Proper refrigerant charge is essential for a system to operate efficiently and safely. A study sponsored by the American Council for an Energy-Efficient Economy (ACEEE) concluded that improper charging of air conditioners and poor maintenance could increase energy use in homes by 20% and waste 17,600 terawatt-hours of energy nationwide every year (Neme et al. 1999). There is a direct link between carbon dioxide production (global warming) and energy efficiency and between leakage of chlorofluorocarbon/hydrochlorofluourocarbon refrigerants and ozone depletion.

A number of investigators have developed methods for detecting low or high refrigerant charges (e.g., Rossi and Braun [1997]; Li and Braun [2007]). However, these methods do not provide an indication of the level of charge. Charge level is very useful information in evaluating whether service is justified and in aiding a technician in adding or removing the appropriate amount of charge during service. The typical approach used to verify refrigerant charge in the field involves the use of either superheat at the evaporator outlet when the expansion device is a fixed orifice or capillary tube and subcooling at the condenser outlet for systems that use variable-area expansion devices. Manufacturers typically provide specifications for superheat or subcooling. However, these specifications are typically not applicable over a wide range of operating conditions (e.g., low or high ambient and high

James E. Braun is a professor in the School of Mechanical Engineering, Purdue University, West Lafayette, IN. **Haorong Li** is an assistant professor in the Department of Architectural Engineering, University of Nebraska-Lincoln, Omaha, NE.

or low mixed-air wet-bulb temperatures) and when faults are present (e.g., low indoor airflow). In addition, the current charge verification protocols utilize compressor suction and discharge pressures to determine refrigerant saturation temperatures that are used to determine evaporator superheat and condenser subcooling. However, the measurement of pressures requires the installation of gauges or transducers that can lead to refrigerant leakage. As a result of these limitations, the current protocols for checking refrigerant charge may be doing more harm than good in many situations.

In order to accurately determine charge level with current practice, technicians would need to evacuate the system and weigh the removed charge. The correct amount of charge would then be added to the system using a scale. This method is very time consuming and costly.

This paper presents a method for obtaining accurate estimates of refrigerant charge level using noninvasive temperature measurements obtained while the system is operating. This method could be used as part of a permanently installed control or monitoring system to indicate charge level and/or to automatically detect and diagnose low or high levels of refrigerant charge. It could also be used as a stand-alone tool by technicians to determine existing charge and during the process of adjusting the refrigerant charge.

The accuracy of the virtual refrigerant charge sensor method is evaluated using laboratory data for a number of different systems and over a wide range of operating conditions with and without the presence of other faults. Seven different systems are considered, including a window unit, residential split systems, and light commercial packaged systems employing either fixed-orifice expansion devices or variable-area expansion devices and R-22 or R-410a as the refrigerant. The virtual refrigerant charge sensor is shown to have good performance in terms of accuracy and robustness. It has the potential to be easily implemented and installed in terms of both hardware and software.

DEVELOPMENT

Refrigerant Charge Indicator

By mass, most of the refrigerant exists as liquid (saturated or subcooled) for normally charged units. In addition, the majority of the refrigerant charge (up to 70%) typically accumulates as liquid in the high-pressure side of the system, including the condenser and liquid line (piping and filter/drier). If there is condenser subcooling, then the liquid line is completely filled with liquid and its liquid volume does not change with refrigerant charge. In addition, the volume of liquid in the two-phase section is relatively constant, because the refrigerant quality varies between 0 and 1 in a nearly linear manner. Therefore, changes in high-side refrigerant charge mostly occur in the subcooled section of the condenser. Furthermore, the volume of liquid within the subcooled section of the condenser is nearly proportional to the amount of subcooling at the exit, T_{sc}, and the liquid density is nearly constant throughout the high-side of the system. With this discussion in mind, the high-side refrigerant charge is related to subcooling using

$$m_{hs} = k_{sc}T_{sc} + m_{hs,0} , \tag{1}$$

where $m_{hs,0}$ is the high-side refrigerant mass for the case of saturated liquid leaving the condenser, k_{sc} is a constant that depends on the condenser geometry, and $m_{hs,0}$ is assumed to be a constant, independent of operating conditions and total charge.

Much less of the total refrigerant charge resides in the low side and, therefore, it is less important to have an accurate characterization of it. Within the low side, most of the refrigerant exists as liquid in the two-phase section of the evaporator and in the sump of the compressor, absorbed within the oil. The volume of liquid within the two-phase section is assumed to be proportional to the total volume of the two-phase section. Furthermore, the volume of the superheat section is nearly proportional to the exit superheat, T_{sh}, and the liquid density is nearly constant throughout the low side of the system. From these considerations, the low-side charge is related to the superheat according to

$$m_{ls} = m_{ls,0} - k_{sh}T_{sh} \ , \tag{2}$$

where $m_{ls,0}$ is low-side refrigerant charge for the case of saturated vapor leaving the evaporator, k_{sh} is a constant that depends on the evaporator geometry, and $m_{ls,0}$ is assumed to be a constant, independent of operating conditions and total charge.

Equations 1 and 2 are applied to any operating condition, including an arbitrary rating condition for the unit, so that

$$m_{hs,rated} = k_{sc}T_{sc,rated} + m_{hs,0} \text{ and} \tag{3}$$

$$m_{ls,rated} = m_{ls,0} - k_{sh}T_{sh,rated} \ , \tag{4}$$

where the subscript *rated* denotes that the rating operating conditions are employed.

Equations 1 through 4 can be combined to eliminate $m_{hs,0}$ and $m_{ls,0}$ and give expressions for changes in subcooling and superheat from rating conditions in terms of changes in charge:

$$k_{sc}(T_{sc} - T_{sc,rated}) = (m_{hs} - m_{hs,rated}) \tag{5}$$

$$-k_{sh}(T_{sh} - T_{sh,rated}) = (m_{ls} - m_{ls,rated}) \tag{6}$$

Equations 5 and 6 can be manipulated to give a single expression that relates subcooling and superheat to the total refrigerant charge:

$$\left(\frac{m_{total} - m_{total,rated}}{m_{total,rated}}\right) = \frac{1}{k_{ch}}\left\{(T_{sc} - T_{sc,rated}) - \frac{k_{sh}}{k_{sc}}(T_{sh} - T_{sh,rated})\right\} \tag{7}$$

where m_{total} is the total refrigerant charge and

$$k_{ch} = \frac{m_{total,rated}}{k_{sc}} \tag{8}$$

Equation 7 provides a direct means of estimating refrigerant charge in terms of measured subcooling and superheat given knowledge of the charge, superheat, and subcooling at an arbitrary rating condition and the constants k_{ch} and k_{sh}/k_{sc}. Equation 7 applies to systems with either fixed or variable throat-area expansion devices. For a system with a fixed-orifice (FXO) expansion device, Equation 7 implies that subcooling must increase when superheat increases for a given refrigerant charge. These directional changes occur with decreasing ambient temperature. For a system with a thermostatic or electronic expansion valve (TXV or EXV), the superheat is relatively constant, so Equation 7 dictates that subcooling is also nearly constant for a given charge. However, when the EXV or TXV is saturated open, the behavior is identical to that for a FXO device. Equation 7 applies for EXV or TXV systems whether or not the valve is operating within range or is saturated open.

For refrigerant charge diagnostic purposes only, it is not necessary to have knowledge of the constant k_{ch} in Equation 7. It is only necessary to evaluate the term within the brackets on the right-hand side of Equation 7, which has the units of temperature and is defined as

$$\Delta T_{sc-sh} = (T_{sc} - T_{sc,\,rated}) - \frac{k_{sh}}{k_{sc}}(T_{sh} - T_{sh,\,rated}) \ . \tag{9}$$

Parameter Estimation

Estimation of k_{sh}/k_{sc}. In Equations 7 and 9, it is necessary to know the ratio of k_{sh} to k_{sc}. This parameter can be determined from data at the rated charge. At the rated refrigerant charge level, Equation 7 reduces to the following:

$$\frac{k_{sh}}{k_{sc}} = \frac{T_{sc} - T_{sc,\,rated}}{T_{sh} - T_{sh,\,rated}} \tag{10a}$$

According to Equation 10a, the ratio of k_{sh} to k_{sc} is the slope of a straight line plot of $(T_{sc} - T_{sc,\,rated})$ versus $(T_{sh} - T_{sh,\,rated})$ for the rated refrigerant charge. In order to evaluate this ratio, it is only necessary to have measurements of superheat and subcooling at the rating condition and a second operating condition. Theoretically, it does not matter what conditions were changed in order to effect a change in subcooling and superheat. It could be a change in condenser inlet temperature or flow rate; evaporator inlet temperature, humidity, or flow rate; or any combination of these variables. However, the result from Equation 10a is very sensitive to the magnitude of the variation in $(T_{sc} - T_{sc,\,rated})$ and $(T_{sh} - T_{sh,\,rated})$ and uncertainties in measurements of T_{sc}, $T_{sc,\,rated}$, T_{sh}, and $T_{sh,\,rated}$. In particular, $T_{sc,\,rated}$ and $T_{sh,\,rated}$ may be estimated from manufacturers' data and could have significant errors. For example, if $T_{sc} = 8 \pm 0.5°\text{C}$, $T_{sh} = 9 \pm 0.5°\text{C}$, $T_{sc,\,rated} = 7 \pm 1°\text{C}$, and $T_{sh,\,rated} = 6 \pm 1°\text{C}$, then $k_{sh}/k_{sc} = 0.33 \pm 0.39$. The uncertainty in k_{sh}/k_{sc} is up to $\pm 118\%$ for this case.

Instead of using manufacturers' rating information, it is advisable to use direct measurements of at least two different conditions at the rated refrigerant charge in order to estimate k_{sh}/k_{sc}. For use of two measurements, Equation 10a can be rewritten as

$$\frac{k_{sh}}{k_{sc}} = \frac{T_{sc,\,1} - T_{sc,\,2}}{T_{sh,\,1} - T_{sh,\,2}} = \frac{\Delta T_{sc}}{\Delta T_{sh}} \ . \tag{10b}$$

Equation 10b eliminates $T_{sc,\,rated}$ and $T_{sh,\,rated}$ and uses two pairs of actual measurements, $(T_{sc,\,1}, T_{sh,\,1})$ and $(T_{sc,\,2}, T_{sh,\,2})$, at the rated refrigerant charge. Since the two pairs of measurements are obtained from the same pair of sensors and the same pair of locations, offset errors can be cancelled and eliminated. In addition, if amplitudes of ΔT_{sc} and ΔT_{sh} are significant, a much more robust k_{sh}/k_{sc} can be obtained from Equation 10b.

Variations in subcooling and superheat would normally be realized by varying a single driving condition, such as condenser airflow, and measuring the response. With this in mind, Equation 10b can be expressed as

$$\frac{k_{sh}}{k_{sc}} = \frac{\Delta T_{sc}}{\Delta T_{sh}} = \frac{\Delta T_{sc}/\Delta dc}{\Delta T_{sh}/\Delta dc} = \frac{k_{sc/dc}}{k_{sh/dc}} \ . \tag{10c}$$

In Equation 10c, *dc* denotes *driving condition*, which could be inlet air conditions or flow rates for the condenser or evaporator. $k_{sc/dc}$ and $k_{sh/dc}$ are slopes of linear functions that relate changes in T_{sc} and T_{sh} to changes in a single driving function. It is best to determine $k_{sc/dc}$ and $k_{sh/dc}$ by varying the driving condition over a wide range, collecting multiple data points, and then performing linear regression. k_{sh}/k_{sc} can be obtained by evaluating $k_{sc/dc}/k_{sh/dc}$. In this manner, offset errors can be eliminated and random errors can be suppressed significantly, so the uncertainty in estimating k_{sh}/k_{sc} is reduced significantly. Among all of the driving conditions, the condenser inlet air temperature (or ambient temperature) is considered to be the best driving condition for estimating k_{sh}/k_{sc} for the following reasons:

1. Refrigerant charge residing in the high-pressure side of the system accounts for the majority of the system charge and, thus, high-side driving conditions have a stronger impact on changes in charge distribution within the system.
2. Variations in ambient temperature are more consistent with the assumptions used in developing the charge algorithm than variations in condenser airflow. An underlying assumption in the derivation of Equation 1 is that for a given heat exchanger, the liquid volume is a unique function of subcooling and vice versa. However, the liquid volume is also a function of condensing temperature minus ambient air temperature (CTOA). For a higher CTOA, the same subcooling degree requires less heat transfer area and, thus, has less liquid volume and mass within the condenser. Since CTOA is reasonably constant for normal operating conditions for a fixed fan speed, the underlying assumption is valid. However, CTOA is inversely proportional to airflow rates. Therefore, under different airflow rates, the same subcooling degree corresponds to slightly different charge levels.

Figure 1 illustrates the dependence of T_{sh} and T_{sc} on condenser inlet air temperature for a split air conditioner with a FXO device as the expansion device and R-410a as the refrigerant. It can be seen that both T_{sc} and T_{sh} decrease linearly with increasing ambient temperatures but with dif-

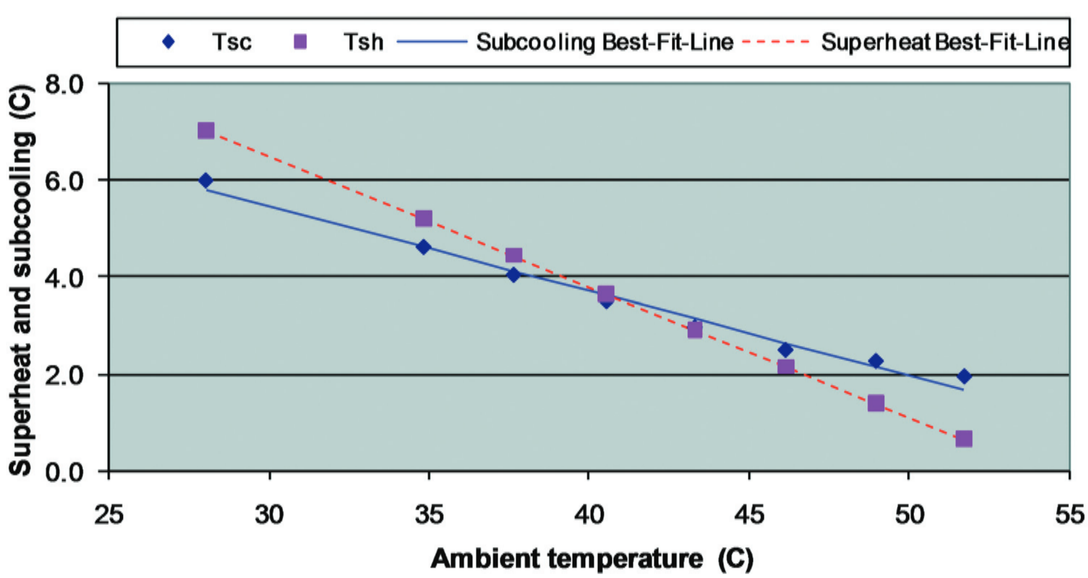

Figure 1. Dependence of T_{sh} and T_{sc} on condenser inlet air temperature for a split air conditioner with an FXO device as the expansion device and using R-410a as the refrigerant.

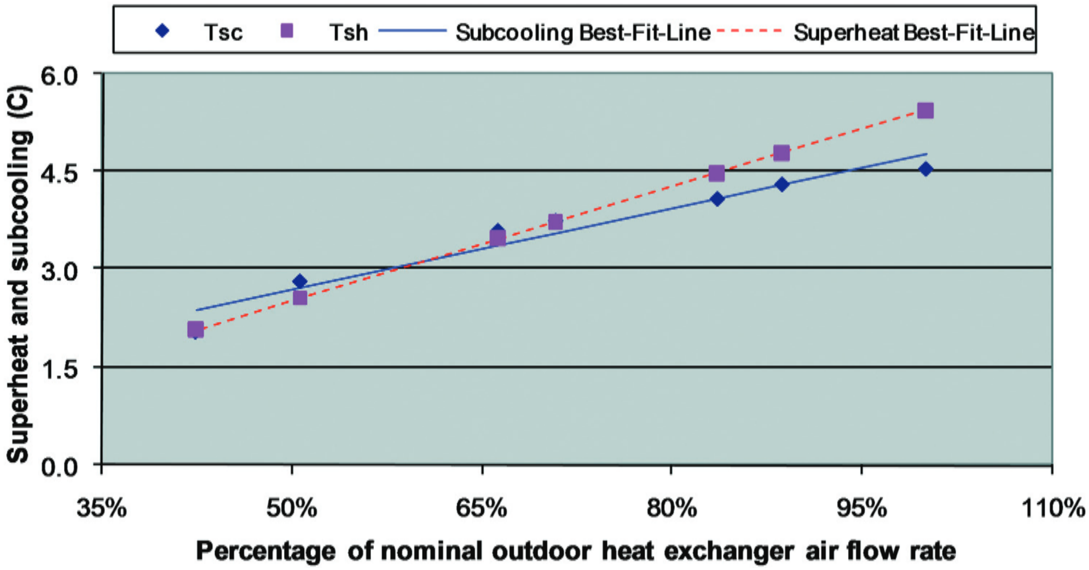

Figure 2. Dependence of T_{sh} and T_{sc} on condenser airflow rates for a split air conditioner with a FXO device as the expansion device and R-410a as the refrigerant.

ferent slopes. The slope ratio, $k_{sc/amb}/k_{sh/amb}$, is equal to 1/1.5. Figure 2 shows the dependence of T_{sh} and T_{sc} on condenser inlet airflow rates for the same system. In this case, the slope ratio, $k_{sc/cfm}/k_{sh/cfm}$, is equal to 1/1.4. This result verifies that k_{sh}/k_{sc} can be obtained under either varying ambient temperatures or varying flow rates (i.e., $k_{sc/amb}/k_{sh/amb} \approx k_{sc/cfm}/k_{sh/cfm}$).

Figure 3 illustrates the linear dependence of T_{sh} and T_{sc} on condenser inlet air temperatures for a packaged air conditioner having a FXO device as the expansion device and R-410a as the refrigerant. In this case, the slope ratio, $k_{sc/amb}/k_{sh/amb}$, is about 1/3.6.

For a system using a TXV as the expansion device, the dependence of T_{sh} and T_{sc} on refrigerant charge levels, condenser inlet air temperatures, and outdoor airflow rates would be different than if the system employed a FXO device as the expansion device. When the TXV is not saturated at a fully open position, T_{sh} only fluctuates around the rating value over a relatively small range, and the refrigerant inventory in the evaporator is relatively constant. In this case, it is not possible to estimate the ratio k_{sh}/k_{sc}, since

$$\frac{k_{sh}}{k_{sc}}(T_{sh} - T_{sh,\,rated}) \approx (T_{sh} - T_{sh,\,rated}) \approx 0 \quad . \tag{11}$$

When a TXV is fully open, it cannot maintain the rated superheat and acts just like a FXO device. Therefore, k_{sh}/k_{sc} could be determined by performing tests under conditions where the TXV is fully opened. However, this is not necessary, since a saturated TXV is an extreme condition and the charge algorithm should determine accurate charge levels under conditions where the TXV is providing superheat control. Consequently, it is sufficient to approximate k_{sh}/k_{sc} as an average value for FXO systems (e.g., 1/2.5).

Estimation of k_{ch}. It is useful to express the parameter k_{ch} in terms of other parameters that have physical meaning where default values can be more easily specified. At the rating condition, the high-side refrigerant of a normally charged system can be expressed as

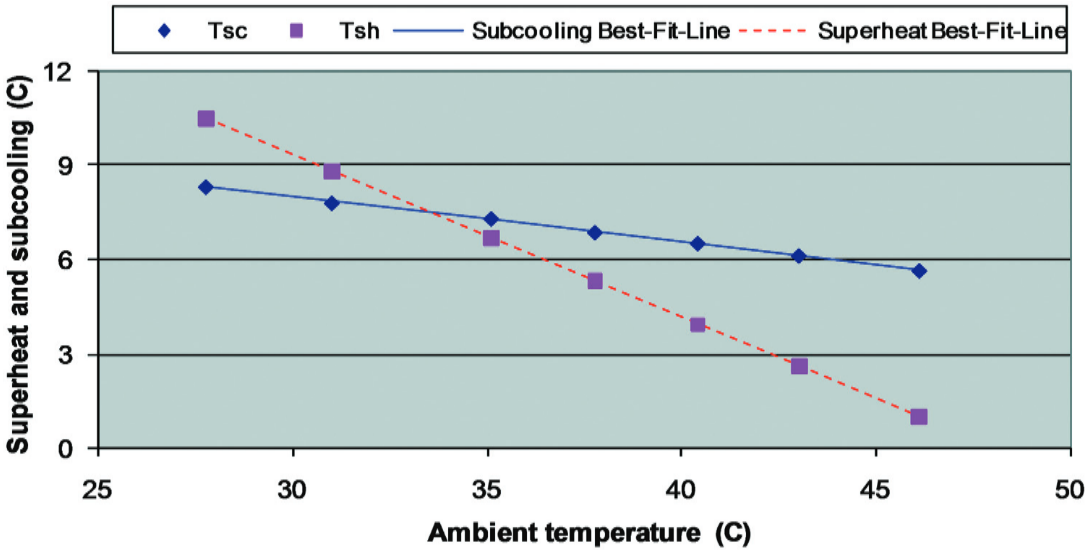

Figure 3. Dependence of T_{sh} and T_{sc} on condenser inlet air temperatures for a packaged air conditioner having a FXO device as the expansion device and R-410a as the refrigerant.

$$m_{hs,\,rated} = X_{hs,\,rated}\, m_{total,\,rated}\ , \tag{12}$$

where $X_{hs,\,rated}$ is defined as the ratio of high-side charge to the total refrigerant charge at the rated charge level and rating operating condition. Assuming that the high-side refrigerant ratio does not change significantly at lower charge levels, then

$$m_{hs,\,o} = X_{hs,\,rated}\, m_{total,\,o}\ , \tag{13}$$

where $m_{hs,\,o}$ and $m_{total,\,o}$ are the high-side refrigerant mass and total refrigerant mass under the condition of saturated liquid at the exit of the condenser, respectively. $m_{total,\,o}$ can then be expressed as

$$m_{total,\,o} = \alpha_o m_{total,\,rated}\ , \tag{14}$$

where α_o is the ratio of refrigerant charge necessary to have saturated liquid exiting the condenser at the rating conditions to the rated refrigerant charge.

Substituting Equations 13 and 14 into Equation 3 leads to

$$k_{ch} = \frac{m_{total,\,rated}}{k_{sc}} = \frac{T_{sc,\,rated}}{(1-\alpha_o)X_{hs,\,rated}}\ . \tag{15}$$

Equation 15 expresses k_{ch} in terms of parameters that have physical meaning and relatively small variations with operating conditions. This allows k_{ch} to be estimated from Equation 15. Harms (2002) conducted detailed laboratory tests to study refrigerant inventory effects that allow good estimates of the parameters on the right-hand side of Equation 15. Table 1 gives values of $X_{hs,\,rated}$ and α_o determined from the data of Harms at rating conditions for three different systems. For these systems, $X_{hs,\,rated}$ ranges from 0.68 to 0.78. These results demonstrate that the majority of the system charge resides in the high side of the system. For the systems considered in Table 1, α_o ranged from 0.70 to 0.82. Generally, these data are not available for specific equipment to be able to determine values of $X_{hs,\,rated}$ and α_o. However, the default values given in Table 1 are the means of the three systems and can be used as reasonable values. These values can then be tuned as outlined in the next section if data are available at different refrigerant charge levels.

IMPLEMENTATION ISSUES

Measurements and Processing

The virtual refrigerant charge sensor requires four measurements at steady-state operating conditions: condensing temperature, liquid-line temperature, evaporating temperature, and suction-line temperature. The two refrigerant saturation temperatures—condensing and evaporating—can be either directly measured using low-cost temperature sensors according to the methods described by Li and Braun (2009) or indirectly derived from saturation pressure measurements.

A steady-state detector is used to filter out the transient data. A combined slope and variance steady-state detection algorithm presented by Li and Braun (2003) is used. This algorithm computes the standard deviation and the slope of the best-fit line through a fixed-length sliding window of recent measurements.

Initial Parameter Estimates

The rated refrigerant charge can be determined from manufacturers' nameplate information or through testing where the system is evacuated and the correct mass of refrigerant is then added to the system. Values for $T_{sc,\,rated}$ and $T_{sh,\,rated}$ can be determined at the rated charge and a rating condition using manufacturers' information or through testing. The rating condition should represent a reasonable average condition for operation of the unit, such as the ARI rating condition of 35°C outdoor air temperature and 26.7°C/19.4°C indoor dry-bulb temperature/wet-bulb temperature (ARI 2006).

For a system with a FXO device, the ratio k_{sh}/k_{sc} should be determined using regression applied to measurements for varying ambient conditions. For a TXV sysem, it is reasonable to employ a value of k_{sh}/k_{sc} equal to 1/2.5.

Based on data available in the literature, a reasonable estimate for $X_{hs,\,rated}$ is 0.73, whereas a value of 0.75 is appropriate for α_o.

Parameter Tuning

The important empirical parameters within the virtual charge sensor algorithm (k_{sh}/k_{sc}, k_{ch}, $T_{sc,\,rated}$, and $T_{sh,\,rated}$) can be tuned to improve accuracy if data is available over a range of

Table 1. $X_{hs,\,rated}$ and α_o for Three Air Conditioners

System	α_o	$X_{hs,\,rated}$
2.5 ton split system	0.73	0.73
5 ton packaged system	0.70	0.78
7.5 ton split system	0.82	0.68
Defaults (rule of thumb)	0.75	0.73

refrigerant charge levels and operating conditions. In this case, errors between predictions of refrigerant charge from Equation 7 and known refrigerant charge can be minimized using regression techniques. The tuning process can be simplified by following a three-step process as follows.

1. Use default values (i.e., initial parameter estimates) for k_{ch}, $T_{sc,\,rated}$, and $T_{sh,\,rated}$ in Equation 7 and use linear regression applied to all of the data to determine the value of k_{sh}/k_{sc} that minimizes errors between predictions and measurements of total refrigerant charge. This step should minimize the scatter in the correlation between predicted and actual charge.
2. Use the value of k_{sh}/k_{sc} from Step 1 and a default value for k_{ch} in Equation 7 and use linear regression applied to data for the rated refrigerant charge only to determine values of $T_{sc,\,rated}$ and $T_{sh,\,rated}$ that minimize refrigerant charge prediction errors. This step should force the correlation between predicted and actual charge to pass through the origin.
3. Use the values of k_{sh}/k_{sc}, $T_{sc,\,rated}$, and $T_{sh,\,rated}$ from Steps 1 and 2 in Equation 7 and use linear regression applied to the all of the data to determine the value of k_{ch} that minimizes refrigerant charge prediction errors. This step should force the correlation between the predicted and actual charges to have the correct slope.

EVALUATION USING LABORATORY DATA

System Descriptions

Harms (2002) tested the effects of charge inventory for three different systems and determined sufficient information to directly calculate parameters for the virtual refrigerant charge sensor. Specifications for the three systems are given in Table 2, and testing conditions are listed in Table 3.

An additional three systems were tested by Shen (2006). However, there was not sufficient information to determine refrigerant charge distribution, so the virtual charge sensor algorithm was evaluated based on both default parameters and parameter tuning methods. System specifications and test operating ranges for these three systems are given in Tables 4 and 5.

Results

Parameters Derived Directly from Measurements. Figures 4, 5, and 6 show performance of the virtual refrigerant charge sensor for data from Harms (2002). In this case, parameters of the algorithm were determined directly from the data. Overall, the agreement between virtual refrigerant charge sensor predictions and actual charge levels is very good. For the 2.5 ton system, four charge levels were tested for one set of operating conditions (Condition A), and the predictions were within ±2%. For the 5 ton system, numerous charge levels were tested for four different operating conditions. In this case, the accuracy was ±10%. Four charge levels with four operating conditions were considered for the 7.5 ton system, and the predictions were within ±4%.

Use of Default Parameters. Figures 7, 8 and 9 show performance of the virtual refrigerant charge sensor for Harms' (2002) data using the default parameters. The performance is slightly worse than when using the parameters derived directly from the measurements. For the 2.5 ton system, the virtual charge predictions are within ±3%. For the 5 ton system, the virtual charge values are within ±9% when the system charge is less than 125%. However, the virtual sensor underestimates charge at very high values and has an error of about –18% for a charge level of 148%. The accuracy for the 7.5 ton system is within ±5%.

Figures 10, 11, and 12 show performance based on default values for the three systems tested by Shen (2006). It can be seen that when the system is not extremely overcharged or undercharged, the virtual sensor based on default parameters has very good performance under a large

Table 2. System Descriptions for Data from Harms (2002)

System	Size, ton	Refrigerant	Expansion Device	Assembling Type	$X_{hs,rated}$, %	α_o
1	2.5	R-407c	TXV	Split	73	0.73
2	5	R-22	TXV	Packaged	78	0.70
3	7.5	R-22	TXV	Split	68	0.82

Table 3. Range of Test Conditions for Data from Harms (2002)

Test Conditions	Air Entering Outdoor Coil	Air Entering Indoor Coil		Refrigerant Charge Level
	Dry-Bulb Temperature, °C	Dry-Bulb Temperature, °C	Wet-Bulb Temperature, °C	% Nominal Charge
A	35.0	26.7	19.7	86–144
B	27.8	26.7	19.7	78–127
C	27.8	26.7	< 13.9	80–148
HT	48.9	26.7	19.4	86–122

Table 4. System Descriptions for Test Data of Shen (2006)

System	Size, ton	Refrigerant Type	Expansion Device	Assembling Type
4	3	R-410a	FXO	Split
5	3	R-410a	FXO	Packaged
6	3	R-410a	TXV	Split

Table 5. Range of Test Conditions for Test Data of Shen (2006)

System	Charge Level, %	Outdoor Flow Rate, %	Indoor Flow Rate, %	Ambient Temperature, °C	Indoor Dry-Bulb Temperature, °C	Indoor Wet-Bulb Temperature °C
4	57–113	35–100	50–100	27–52	27	16–24
5	58–130	100	45–130	27–52	27	12–23
6	61–141	32–100	50–140	27–52	27	12–23

variation of ambient driving conditions and severe faulty conditions such as low indoor or outdoor airflow rates. However, when the system is extremely overcharged or undercharged, the virtual sensor may have significant errors. For example, the virtual sensor predicts –58% of nominal charge when the system is charged at –43% for the 3 ton split FXO and R-410a system. Fortunately, this is not a problem as long as the virtual sensor can provide accurate results when the system is close to the proper charge (±20%). The accuracy of the sensor is not critical when the system charge levels are extremely high or low because, typically, actions should be taken before the charge level drops to –20% due to significant degradation in the cooling capacity and efficiency.

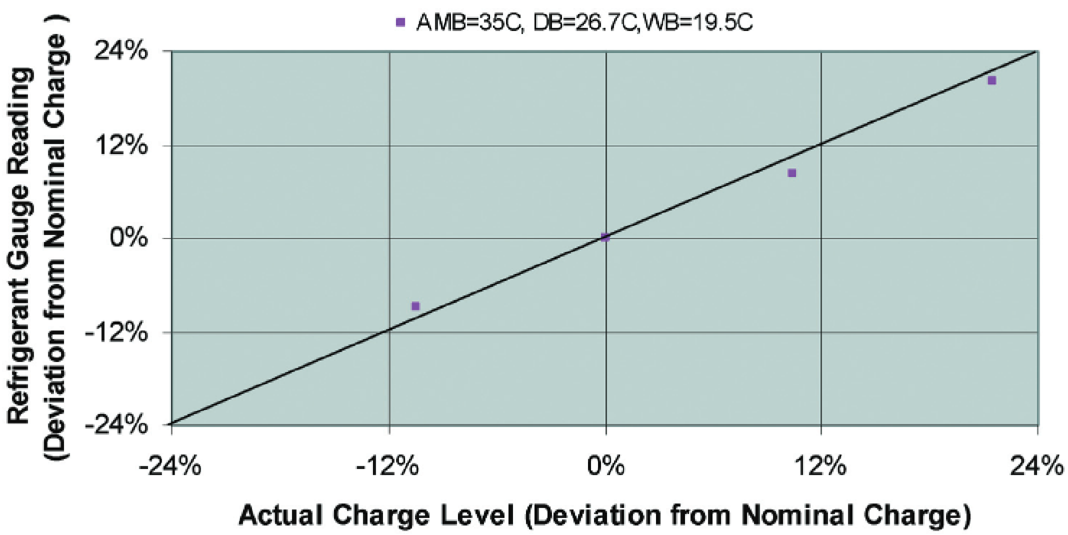

Figure 4. Virtual refrigerant charge sensor performance for a 2.5 ton split TXV and R-410a system for parameters derived directly from Harms' (2002) data.

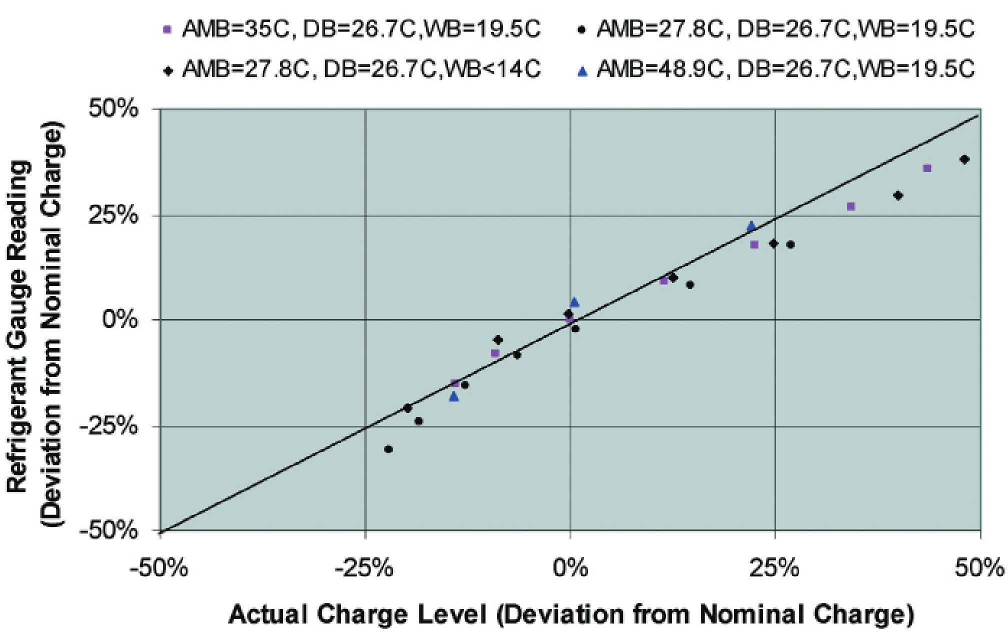

Figure 5. Virtual refrigerant charge sensor performance for a 5 ton split TXV and R-22 system for parameters derived directly from Harms' (2002) data.

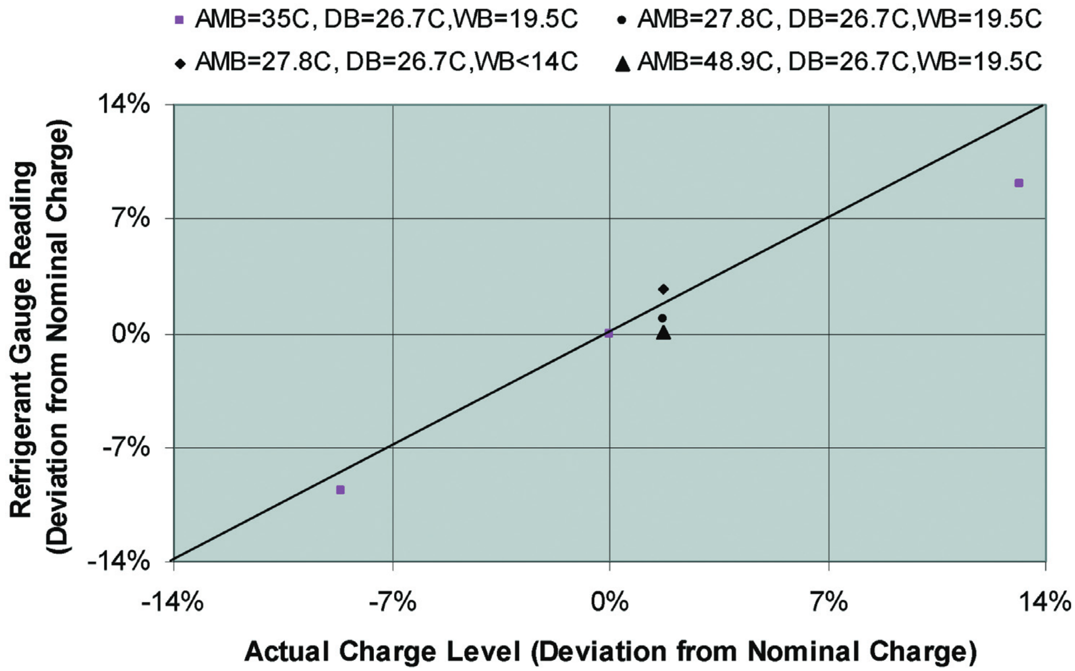

Figure 6. Virtual refrigerant charge sensor performance for a 7.5 ton split TXV and R-22 system for parameters derived directly from Harms' (2002) data.

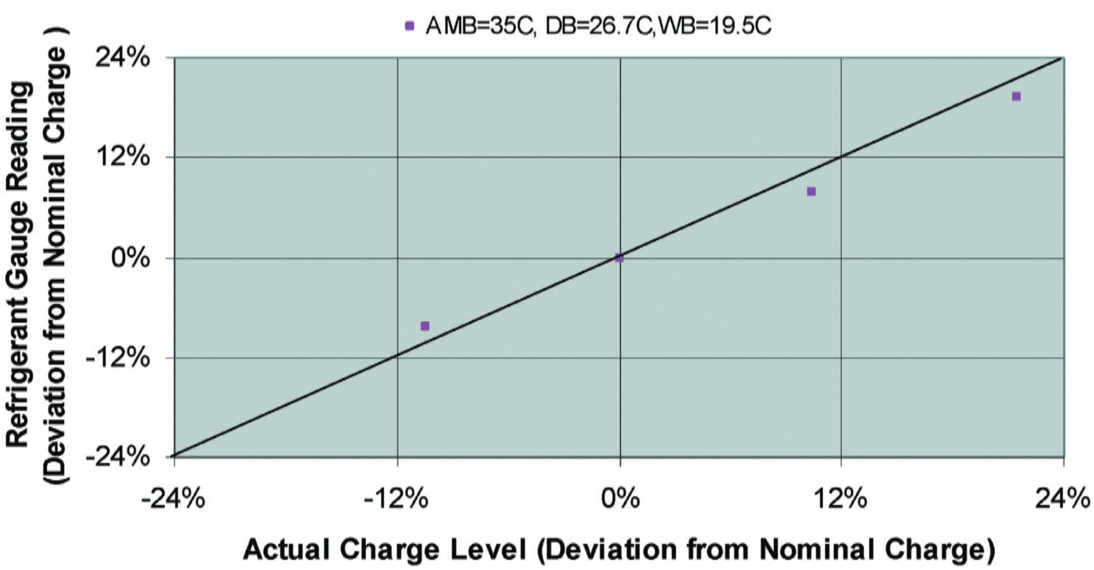

Figure 7. Virtual refrigerant charge sensor performance for a 2.5 ton split TXV and R-410a system tested by Harms (2002) and based on default parameter values.

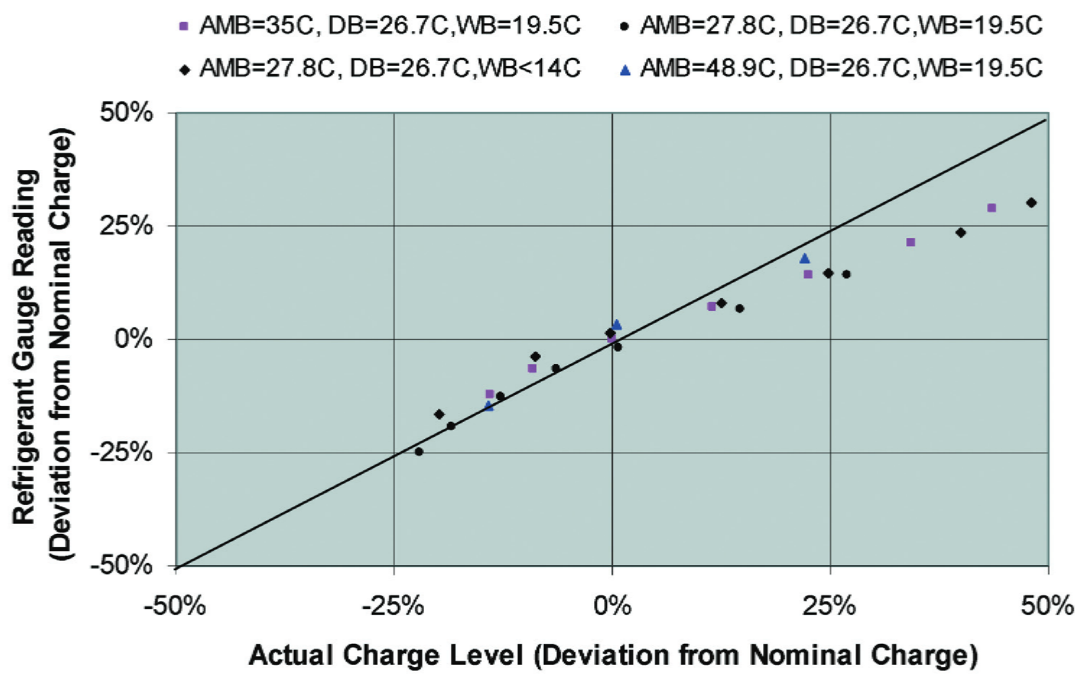

Figure 8. Virtual refrigerant charge sensor performance for a 5 ton split TXV and R-22 system tested by Harms (2002) and based on default parameter values.

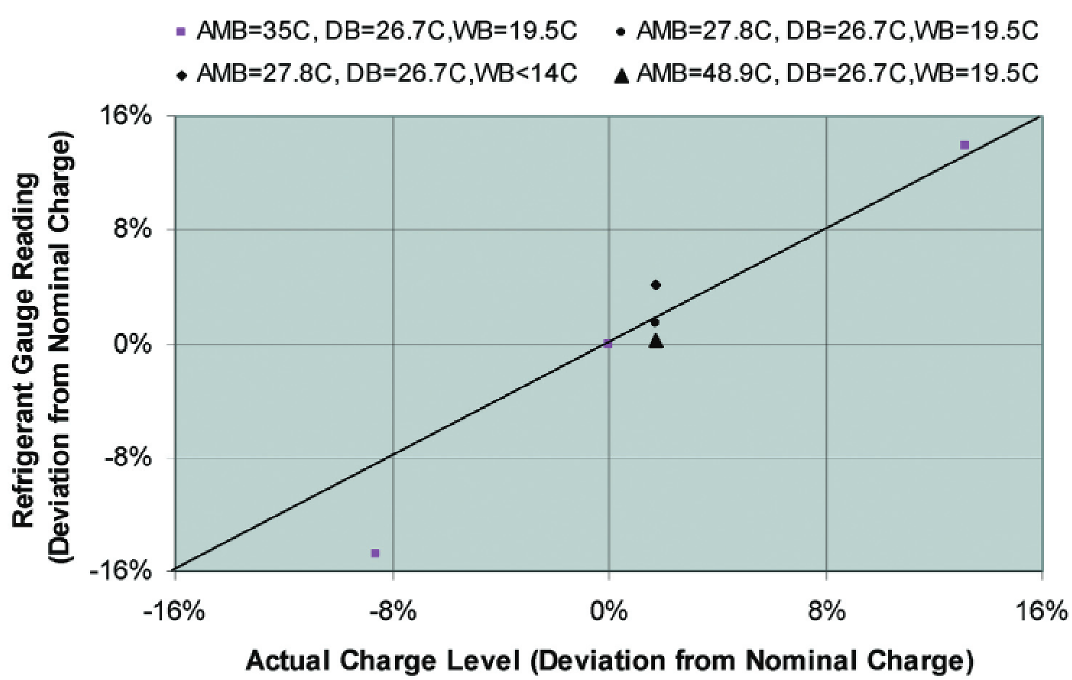

Figure 9. Virtual refrigerant charge sensor performance for a 7.5 ton split TXV and R-22 system tested by Harms (2002) and based on default parameter values.

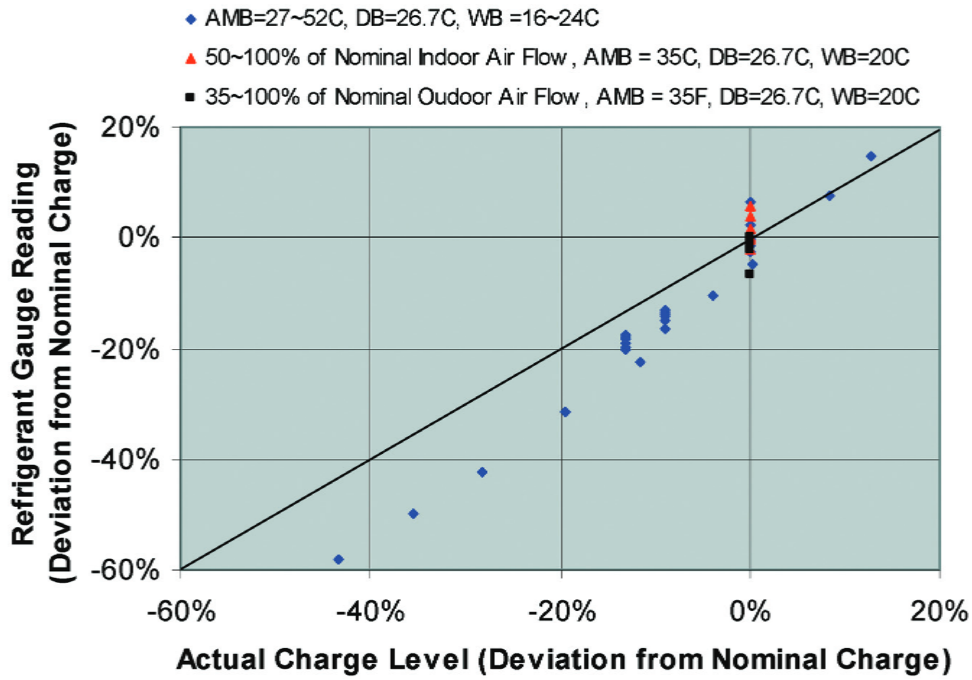

Figure 10. Virtual refrigerant charge sensor performance for a 3 ton split FXO and R-410a system tested by Shen (2006) and based on default parameters.

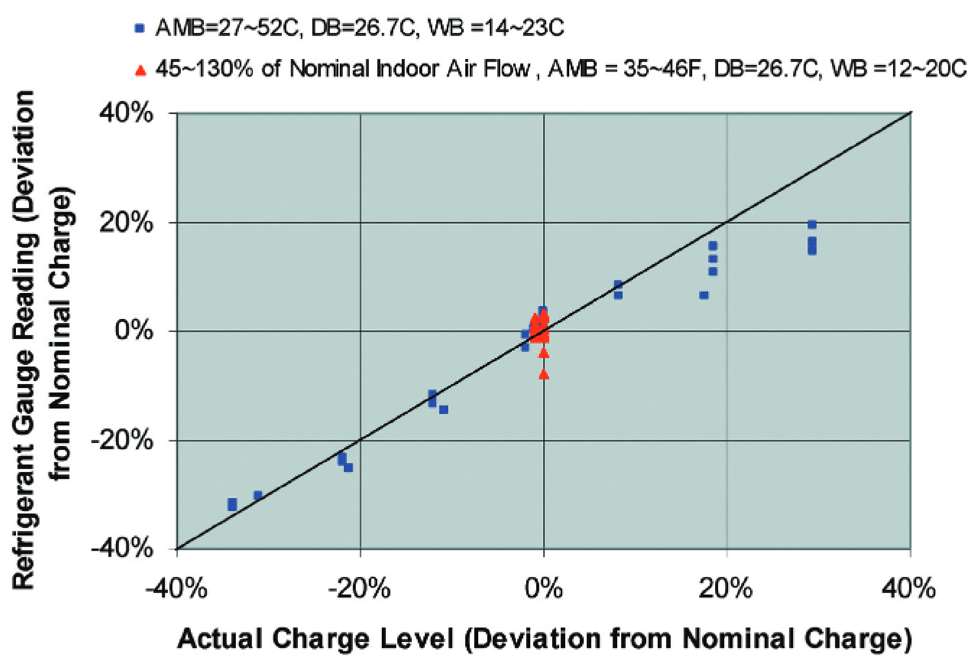

Figure 11. Virtual refrigerant charge sensor performance for a 3 ton packaged FXO and R-410a system tested by Shen (2006) and based on default parameters.

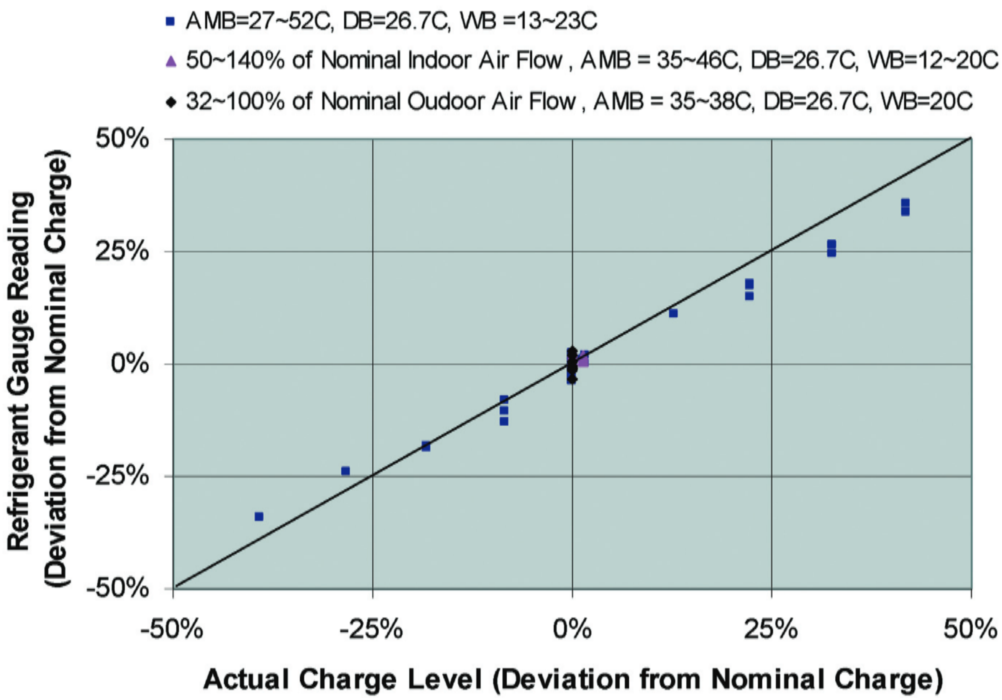

Figure 12. Virtual refrigerant charge sensor performance for a 3 ton split TXV and R-410a system tested by Shen (2006) and based on default parameters.

Use of Tuned Parameters. Figures 13–15 show performance for the three systems tested by Shen (2006) with the parameters tuned using the measured data. There is a significant improvement compared to using default parameters, and predictions are accurate over the entire large range of charge levels under large variations of ambient driving conditions and in the presence of other severe fault conditions such as low indoor and outdoor airflow rates. Table 6 summarizes differences in performance between using default and tuned parameters.

PROTOTYPE DEMONSTRATION

A prototype of the virtual refrigerant charge sensor was developed and implemented within a personal data assistant (PDA) platform. The system was then applied to a small window air conditioner. The system has a cooling capacity of 5200 Btu, uses R-22 as the refrigerant, and uses a fixed-orifice expansion device. The nominal charge is 9 oz, and its rated subcooling and superheat are 6.7°C and 4.5°C, respectively.

As shown in Figure 16, four thermocouples were mounted on the outer surface of the refrigerant tubing and were insulated using sticky foam. Temperature measurements were acquired using a simple commercially available acquisition board. Algorithms for the steady-state detector and charge level determination were implemented within the PDA. During testing, refrigerant was recovered from the system using a refrigerant recovery machine and weighed using a scale. The virtual charge readings were displayed on the PDA.

Due to the lack of detailed physical information for the system, default values for parameters of k_{ch} and k_{sh}/k_{sc} were used. Figure 17 compares virtual and actual charge levels. This system could only operate under charge levels ranging from 70% to 130% of nominal charge level

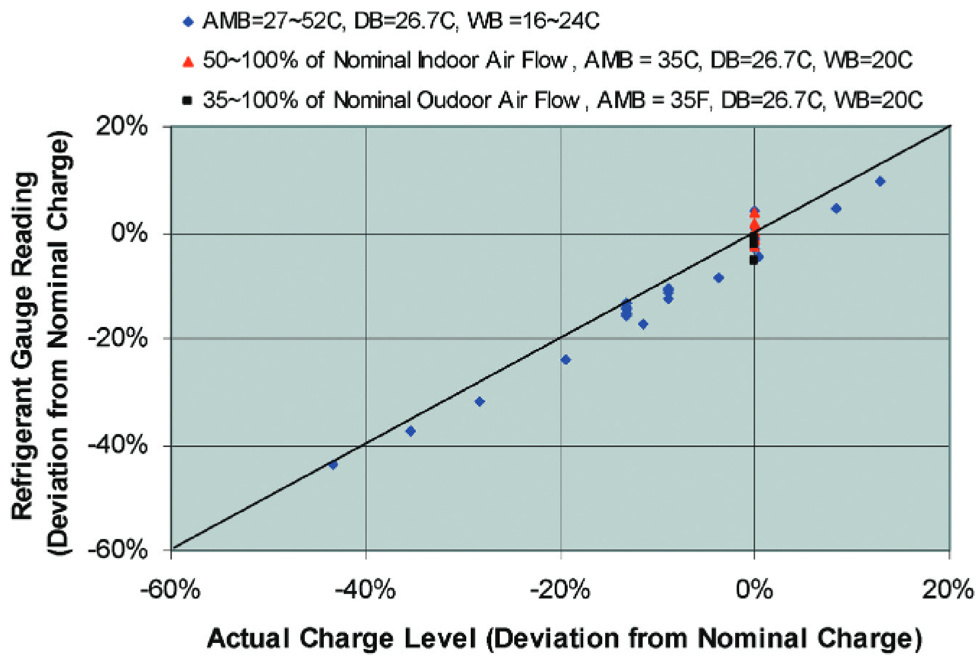

Figure 13. Virtual refrigerant charge sensor performance for a 3 ton split FXO and R-410a system tested by Shen (2006) and based on tuned parameters.

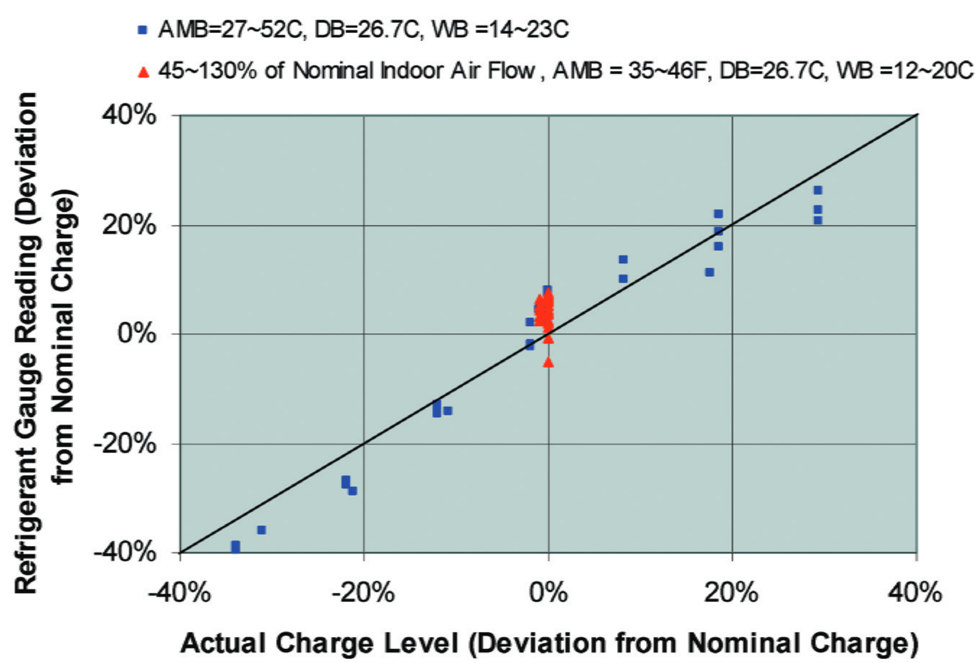

Figure 14. Virtual refrigerant charge sensor performance for a 3 ton packaged FXO and R-410a system tested by Shen (2006) and based on tuned parameters.

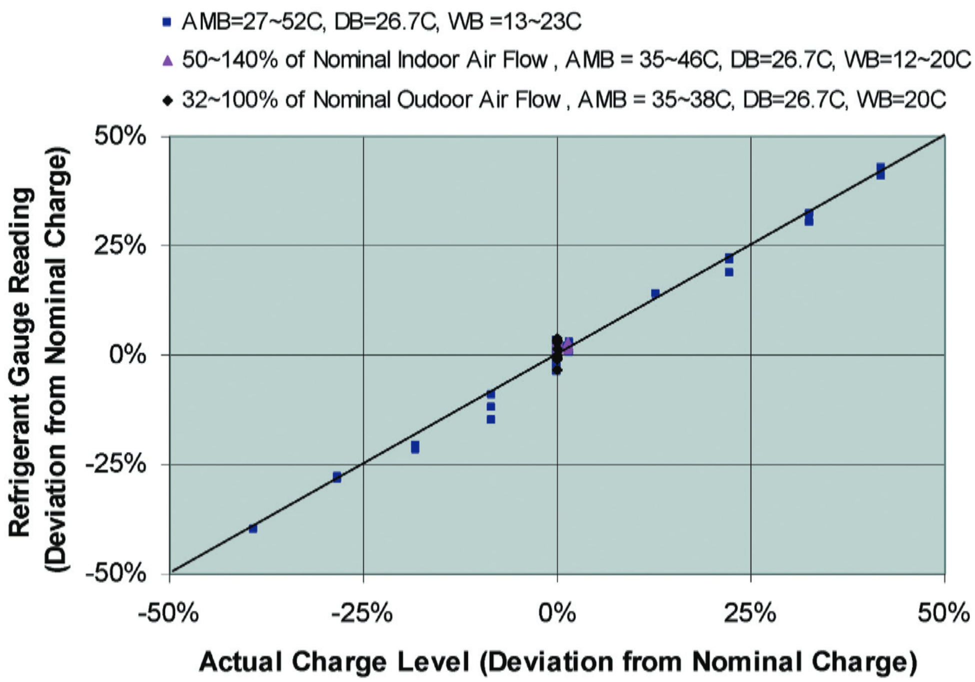

Figure 15. Virtual refrigerant charge sensor performance for a 3 ton split TXV and R-410a system tested by Shen (2006) and based on tuned parameters.

Table 6. Comparison of Performance Using the Default and Tuned Parameters

System	Error	
	Default Parameters	Tuned Parameters
4	–15%–6%	–5%–4%
5	–15%–3%	–8%–7%
6	–8%–2%	–7%–3%

without shutting down due to low- or high-pressure cutouts. For each charge level, simulated evaporator and condenser fouling were introduced into the system to test its robustness. Evaporator and condenser fouling were simulated by using sheets of paper to block airflow through portions of these heat exchangers. A total of 36 test points were collected and plotted in Figure 17. It can be seen that the charge sensor has good accuracy under various operating and faulty conditions.

SUMMARY

Development and evaluation of a virtual refrigerant charge sensor was presented. Seven different systems were considered in the evaluation, covering both small and large cooling capacities, including a window unit, residential split systems, and light commercial packaged systems, incorporating both fixed-orifice expansion devices and variable area expansion devices, and employing R-22 or R-410a. Overall, with parameters of the sensor determined or tuned from measured data, the virtual refrigerant charge sensor

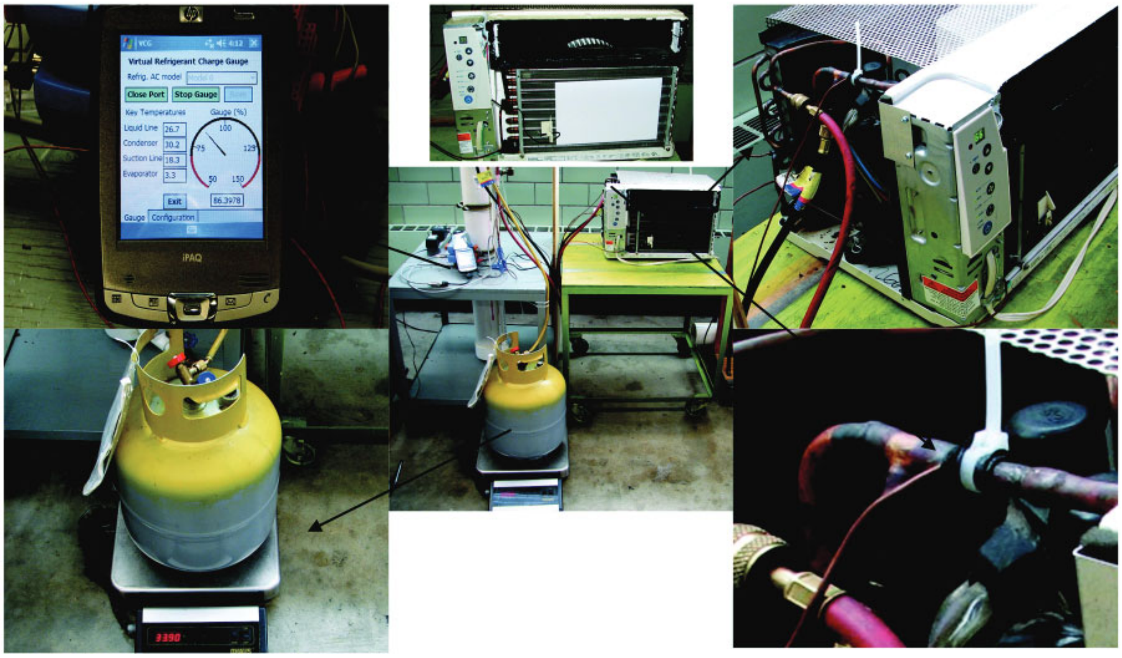

Figure 16. Prototype demonstration.

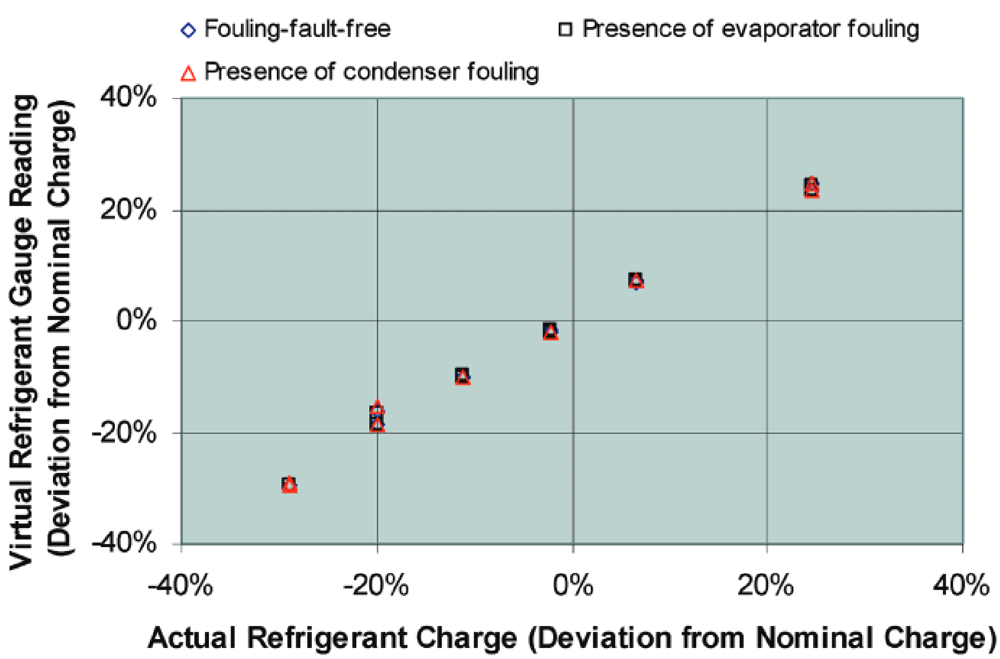

Figure 17. Virtual refrigerant sensor performance for a window FXO and R-22 system.

1. has very good performance in terms of accuracy (ranging from ±3% to ±10%),
2. is very robust against both variations in operating conditions and impacts of other faults,
3. can be easily implemented at low costs in terms of both hardware and software, and
4. is generic for both TXV and FXO systems.

The algorithm can be readily implemented using default values provided in the paper. Particularly, the default parameters work better for TXV systems (with an error ranging from –8% to 7%) than for FXO systems (with an error ranging from –15% to 6%). Although the performance of the algorithm based on default parameters is not as good as that of derived or tuned parameters, it is reasonably good. The default parameters are not meant to replace derived or tuned parameters but to provide a starting point for future training and learning.

In terms of applications, the sensor could be used as part of a permanently installed control or monitoring system to indicate charge level and/or to automatically detect and diagnose low or high levels of refrigerant charge. It could also be used as a stand-alone tool by technicians to determine existing charge during the process of adjusting the refrigerant charge.

ACKNOWLEDGMENTS

This work was co-supported by the California Energy Commission, the U.S. Department of Energy, Purdue Research Foundation, and the University of Nebraska-Lincoln.

NOMENCLATURE

k = slope of the best-fit line geometry constant
m = mass of charge, kg
T = temperature,°C
X = quality
α_o = ratio of refrigerant charge necessary to have saturated liquid exiting the condenser at the rating conditions to the rated charge

Subscripts

ch = charge
hs = high side
ls = low side
0 = zero-subcooling or superheat
rated = nominal value at rated conditions
ref = refrigerant
sc = subcooling
sh = superheat
suc = suction line temperature
total = total value
sh/dc = partial differential of superheat to a certain driving condition
sc/dc = partial differential of subcooling to a certain driving condition

REFERENCES

ARI. 2006. *ARI Standard 210-240, Standard for Performance Rating of Unitary Air Conditioning and Air Source Heat Pump Equipment.* Arlington, VA: Air Conditioning and Refrigeration Institute.

Cowan, A. 2004. Review of recent commercial rooftop unit field studies in the Pacific Northwest and California. Northwest Power and Conservation Council and Regional Technical Forum, October 8, Portland, OR.

Harms, T.M. 2002. Charge inventory system modeling and validation for unitary air conditioners. PhD thesis, School of Mechanical Engineering, Purdue University, West Lafayette, IN.

Li, H., and J.E. Braun. 2003. An improved method for fault detection and diagnosis applied to packaged air conditioners. *ASHRAE Transactions* 109(2):683–92.

Li, H., and J.E. Braun. 2007. A methodology for diagnosing multiple-simultaneous faults in vapor compression air conditioners. *HVAC&R Research* 13(2):369–95.

Li, H., and J.E. Braun. 2009. Virtual refrigerant pressure sensors for use in monitoring and fault diagnosis of vapor compression equipment. *HVAC&R Research*, forthcoming.

Neme, C., J. Proctor, and S. Nadel. 1999. Energy savings potential from addressing residential air conditioner and heat pump installation problems. Report No. A992, American Council for an Energy Efficient Economy, Washington, DC.

Proctor, J., and T. Downey. 1995. Heat pump and air conditioner performance. Affordable Comfort Conference, March 26–31, Pittsburgh, PA.

Rossi, T.M., and J.E. Braun. 1997. A statistical, rule-based fault detection and diagnostic method for vapor compression air conditioners. *HVAC&R Research* 3(1):19–37.

Shen, B. 2006. Improvement and validation of unitary air conditioner and heat pump simulation models at off-design conditions. PhD thesis, Herrick Laboratories, Purdue University, West Lafayette, IN.